Nov 13th, 12:00 AM

Stress Concentrations in the Joints of a Ladder Frame Subjected to Torsion

J. Ergatoudis

T. H. G. Megson

M. H. Datoo

Seventh International Specialty Conference on Cold-Formed Steel Structures
St. Louis, Missouri, U.S.A., November 13-14, 1984

STRESS CONCENTRATIONS IN THE JOINTS OF A LADDER FRAME SUBJECTED TO TORSION

T. H. G. Megson, J. Ergatoudis and M. H. Datoo

1. INTRODUCTION

It has previously been shown (4, 5) that stresses and displacements in the thin-walled open section secondary beams of a ladder frame (Fig. 1) subjected to torsion may be accurately determined along the length of the beam by the use of a 'warping restraint factor' which is found, for a particular joint configuration, by a finite element analysis.

A subsequent finite element investigation of joints comprising channel section main beams and channel or I-section secondary beams has shown that the distribution of stress in the immediate vicinity of the partially restrained end of the secondary beam is not linear as predicted by the theory of references (4, 5), but varies such that stress concentrations occur at flange tips. Furthermore these stress concentrations are not only functions of the applied torque but vary with the thickness of the restraining plate (i.e. the main beam web) reaching a maximum at a specific plate thickness, this maximum being greater than the stress produced by complete warping restraint. The existence of these stress concentrations is verified using perspex models. In addition it is shown both theoretically (finite element analysis) and experimentally that, in joints fabricated from mild steel components, fillet welding the connection does not eliminate these stress concentrations but merely transfers them to the toe of the weld.

Also, although generally in thin-walled theory secondary warping effects are assumed to be negligible, it is shown that they are significant in some cases of complete and partial warping restraint. Expressions for secondary warping and the associated constraint stresses have been developed and shown to give good agreement with finite element values at sections away from the restrained end. At this section it is necessary to use the finite element technique to predict stresses and displacements and these are shown to agree closely with measured values.

Finally, recommendations based on the above investigation are made to enable designers to select sections which reduce stress concentrations to a minimum for a given torque loading.

T. H. G. Megson, Senior Lecturer in Civil Engineering, University of Leeds
J. Ergatoudis, Lecturer in Civil Engineering, University of Leeds
M. H. Datoo, Late of the Department of Civil Engineering, University of Leeds

2. FINITE ELEMENT ANALYSIS

The finite element analysis in this research was carried out using subroutines from the Program for Automatic Finite Element Calculation known as PAFEC (7). The output from the program lists values of displacement and rotation at element nodes and, if required, stresses.

2.1. Joint Idealisation

All the joints investigated were idealised using eight node isoparametric quadrilateral elements which combine both bending and membrane properties. A typical idealisation is shown in Fig. 2 where a channel section secondary beam is attached to the web of a channel section main beam. Since such a joint is antisymmetric only half need be considered.

The finite element mesh was graded in the vicinity of the joint to enable accurate values of stress to be determined in a region of high stress gradient. A problem arose, however, in that at the flange tip/main beam junction a theoretical singularity occurs such that finite element stress values do not converge as the mesh size decreases. This was overcome by determining stress distributions for a range of mesh sizes and selecting the one in which the values of stress at a node shared by two elements differed by less than ten per cent, a figure generally accepted as a measure of the accuracy of an idealisation.

2.2. Stress Oscillations

The output from the finite element analysis lists values of displacement and stress at the mid-plane and the inner and outer surfaces of each element at its nodal points. Since, in an experimental investigation, it is only possible to measure surface stresses it is the finite element surface stresses which must be used for comparison purposes. It was found, however, that in the vicinity of the connection these stresses oscillated round the profile of the secondary beam as shown, for the flange of an I-section beam in Fig. 3. A true value of surface stress can be found by drawing the separate envelopes for the 'peaks', corresponding to the element mid-side nodes, and the 'troughs', corresponding to the element corner nodes, and then finding the mid-line. A difficulty arises in extrapolating the 'peak' envelope to the flange tip since this is a region of high stress gradient. It was decided, therefore, that in all cases the stress values at the two mid-side nodes before the flange tip would be extrapolated linearly to the flange tip; the surface stress at the flange tip is then the mean of this value, σ_m in Fig. 3, and that, σ_c, obtained from the flange tip corner node.

2.3. Stress Redistribution

A finite element analysis was carried out on a range of joint configurations comprising both channel and I-section secondary beams and channel section main beams of varying web thickness. Fig. 4. shows the variation of mid-plane direct stress round the profile of a channel section secondary beam at three stations along the beam; included also are the distributions predicted by the theory of references (4, 5). At the built-in end (Fig. 4(a)) the finite

element analysis predicts a stress concentration at the flange tip but this rapidly decreases with distance from the built-in end so that at z = 20 mm (Fig. 4(c)) the stress distributions are practically identical.

Fig. 5 shows the variation of the secondary beam mid-plane flange tip direct stress with main beam web thickness at the built-in end. The finite element analysis predicts that this stress increases initially with decreasing web thickness reaching a maximum at a main beam web thickness which is equal to the secondary beam thickness; the stress falls rapidly with further decreases in main beam web thickness. It can be seen that this maximum value of stress is approximately 2.8 times the value predicted by basic theory (3) for the case of completely restrained warping.

2.4. Idealisation of Fillet Welds

The stress distributions in the immediate vicinity of the joint connections were investigated experimentally using glued perspex and, more realistically, fillet welded mild steel models of joints. It was clear in the latter case that the fillet welds would have a marked effect on the stress distribution at the built-in end. A method was therefore required of simulating the fillet welds in the finite element analysis so that a direct comparison could be made.

The elements used in the simulation were two-dimensional, triangular, six node bending-membrane elements of sufficient number and thickness so that, when placed side by side, they represented completely the fillet weld round the profile of the secondary beam; a typical arrangement is shown in Fig. 6.

Fig. 7. shows mid-plane flange tip direct stress distributions for a channel section secondary beam, with and without fillet welds, at the built-in end and at the toe of the weld. It can be seen that while the weld reduces the direct stress to virtually zero at the built-in end, it has no effect on the stress redistribution at the toe of the weld. Furthermore, the stress concentration at the toe of the weld is only slightly reduced from that at the built-in end when no weld is present.

3. SECONDARY WARPING EFFECTS

Generally open sections in which the ratio *maximum thickness/typical cross-sectional dimension* < 0.1 are regarded as thin-walled so that secondary warping effects, i.e. effects associated with warping across the wall thickness, are assumed to be negligible. In some sections, however, although the condition is satisfied, the assumption has been found to be invalid particularly when the flange width is large compared with the web depth.

Oden (6) and Gjelsvik (2) have investigated secondary warping of open sections. However, Oden only considered sections which do not experience primary warping such as thin rectangular section bars, angle and tee-sections while Gjelsvik determined the secondary warping distribution round an I-section by considering it to be an assemblage of three separate thin rectangular section bars thereby neglecting primary warping.

In this section methods are proposed for determining combined primary and secondary warping effects for sections subjected to free, completely restrained and partially restrained warping.

3.1. Free Warping

The complete derivation of the expression for the warping of any point in the cross-section of a thin-walled open section beam is given in reference (1). Here, for brevity, the result is quoted and is

$$w = -2A_R \frac{d\theta}{dz} + ns_s \frac{d\theta}{dz} \qquad (1)$$

The first term on the right hand side of eqn.(1) is the free primary warping of the section while the second term gives the free secondary warping. Also, in eqn.(1), $d\theta/dz = T/GJ$ which is constant in the free warping case.

3.2. Completely Restrained Warping

In the case where one end of the beam is completely restrained against warping eqn.(1) still holds although $d\theta/dz$ is no longer constant but is given by (3)

$$\frac{d\theta}{dz} = \frac{T}{GJ}\left[1 - \frac{\cosh \mu(L - z)}{\cosh \mu L}\right] \qquad (2)$$

The associated direct stress system is, from Hooke's law

$$\sigma_\Gamma = E \frac{\partial w}{\partial z} \qquad (3)$$

Substituting in eqn.(1) for $d\theta/dz$ from eqn.(2) and then in eqn.(3) for w gives

$$\sigma_\Gamma = -2A_R E \frac{T}{GJ} \mu \frac{\sinh \mu(L-z)}{\cosh \mu L} + Ens_s \frac{T}{GJ} \mu \frac{\sinh \mu(L-z)}{\cosh \mu L} \qquad (4)$$

where the first and second terms on the right hand side of eqn.(4) are expressions for the direct stress systems corresponding to completely restrained primary and secondary warping respectively.

Further the shear stress associated with the direct stress system of eqn.(4) is given by (3)

$$\tau_\Gamma = -\frac{1}{t} \int_o^s t \frac{\partial \sigma_\Gamma}{\partial z} \, ds \qquad (5)$$

or, substituting in eqn.(5) from eqn.(4)

$$\tau_{\Gamma} = -E \frac{T}{GJ} \frac{\mu^2}{t} \frac{\cosh \mu(L-z)}{\cosh \mu L} \int_0^s 2A_R \, t \, ds + Ens_s \frac{T}{GJ} \frac{\mu^2}{t} \frac{\cosh \mu(L-z)}{\cosh \mu L} \int_0^s t \, ds \qquad (6)$$

The total shear stress at any point in the cross-section is the sum of the St. Venant shear stress and τ_{Γ}, i.e.

$$\tau = \tau_{St.V} + \tau_{\Gamma} \qquad (7)$$

where

$$\tau_{St.V} = \pm 2n \frac{T}{J} \qquad \text{(ref. (3))} \qquad (8)$$

Direct and shear stress distributions round the profile of a channel section secondary beam were determined at a section some distance from the completely restrained end using eqns. (4), (6), (7) and (8). The results were compared with a finite element analysis and, as can be seen from Figs. 8 and 9, good agreement was obtained.

3.3. Partially Restrained Warping

It has been shown (4) that direct and shear stress systems in an open section beam subjected to partial warping restraint at one end are related to the completely restrained case as follows

$$\sigma_p = (1 - k)\sigma_{\Gamma} \qquad (9)$$

$$\tau_p = (1 - k)\tau_{\Gamma} \qquad (10)$$

in which k is the warping restraint factor (4) and σ_{Γ} and τ_{Γ} are given by eqns. (4) and (6) respectively.

4. EXPERIMENTAL INVESTIGATION

Generally in finite element analysis the accuracy of values of stress obtained at nodes common to two or more elements in different planes is open to doubt. Since this is the situation at the partially built-in end of a secondary beam it was decided to verify the predicted stress redistributions and concentrations experimentally.

4.1. Glued Perspex Joints

Initially model ladder frame joints were constructed from perspex and comprised channel section secondary beams glued to perspex sheets representing the main beam web. Channel section secondary beams were used in preference to I-section since they were easier to fabricate and represented the more

complex case. Electrical resistance strain gauges were attached at intervals round the profile of the secondary beam as close as possible to the main beam web. A torque was applied to the free end of the secondary beam in the form of a couple acting on a plate which was freely slotted over the end of the beam. This arrangement, shown diagrammatically in Fig. 10, allowed unrestrained warping of the free end of the secondary beam while minimising local effects due to load application.

Torsion tests were carried out on models having main web thicknesses of 4 mm, 6 mm, 10 mm and 12 mm; in all cases the secondary beam had a uniform thickness of 6 mm.

Fig. 11 shows stress distributions at the built-in end of a secondary beam attached to a main beam web of thickness 4 mm. Close agreement is obtained between finite element and experimental results while the theoretical values predicted by eqn.(4) are in very poor agreement with the measured values.

4.2. Welded Steel Joints

Six joints were constructed using channel section secondary beams fillet welded to plates representing the main beam webs. Three secondary beams, each having a uniform thickness of 3 mm, were welded to plates of thickness 1.5 mm, 3 mm and 5 mm respectively while the remaining three secondary beams, each 6 mm thick, were welded to plates 3 mm, 6 mm and 12 mm thick. In all cases the welds had a leg length of 6 mm.

Electrical resistance strain gauges were attached to all secondary beams at intervals round the profile of each beam section on its outside surface and as close to the toe of the weld as possible. Each joint was placed in turn in a torsion machine which allowed the free end of the secondary beam to warp without restraint and in which the plate was supported such that rotation was allowed along all of its four edges, i.e. simple support conditions.

Fig. 12 shows the distribution of direct stress in a secondary beam at the toe of the weld obtained experimentally, by finite element analysis and by the theory of eqn.(4). Good agreement is obtained between experimental and finite element results while eqn.(4) is seen to be inapplicable in this region.

5. DESIGN CONSIDERATIONS

A parameter study was undertaken in which main and secondary beam dimensions were varied to determine their effect; if any, on the magnitude of the stress concentration at flange tips; combinations of channel section main beams and channel and I-section secondary beams were considered.

5.1. Stress Concentration Factor

To enable the effects of the different beam dimensions on the stress concentrations at flange tips to be studied more easily a stress concentration factor (SCF) was defined such that

$$SCF = \frac{\sigma_p \text{ (finite element value at flange tip)}}{\sigma_T \text{ (at flange tip using eqn.(4))}}$$

5.2. Parameter Study

Finite element analyses were carried out on two groups of joints, one group having channel section secondary beams the other I-section secondary beams. In each case a joint having typical practical dimensions was chosen and then each of the variables t_s, t_f, t_w, b, d and R_d was varied in turn over a range of values whilst the remaining variables were constant. Figs. 13(a) and (b) show the variation of SCF with R_d for an I- and a channel section secondary beam respectively.

5.3. Design Recommendations

The variation of SCF with each of the variables specified in Section 5.2. is shown in graphical form for the complete range of joint geometries in reference (1). Typical is the variation of SCF with R_d shown in Figs. 13(a) and (b). From these graphs it can be seen that the SCF is a minimum, i.e. the mid-plane and surface stresses have the same value, when R_d is in the range 1.3 - 1.4.

Based on the parameter study detailed in reference (1) the following additional recommendations are made:-

The main beam web thickness should be approximately 1.75 times the secondary beam thickness.

The flange width to web depth ratio should be in the range 0.2 - 0.3.

The SCF increases rapidly with flange width for both channel and I-section secondary beams being of the order of 3.0 when the flange width is equal to the web depth. Thus the flange width should be kept as small as possible and in the range specified above.

6. CONCLUSIONS

It has been shown theoretically, using finite element analysis, that stress concentrations occur in the joints of a ladder frame subjected to torsion; the existence of these stress concentrations has been verified experimentally. It has also been shown that existing theory, while giving good agreement with measured values at sections away from the partially restrained end, is inapplicable in the immediate vicinity of a joint. Furthermore, the presence of fillet welds does not eliminate these stress concentrations but merely transfers them to the toe of the weld.

Modifications to existing theory to allow for the effects of secondary warping have been proposed and shown to give good agreement with finite element values at sections at some distance from the partially restrained end.

APPENDIX 1: References

1. Datoo, M. H., "Stress Concentrations in the Joints of a Ladder Frame Subjected to Torsion", Thesis submitted in partial fulfilment of the requirements for Ph.D., University of Leeds, 1983.

2. Gjelsvik, A., "The Theory of Thin Walled Bars", John Wiley and Sons, New York, 1981.

3. Megson, T. H. G., "Aircraft Structures for Engineering Students", Edward Arnold, London, 1972.

4. Megson, T. H. G. and Alade, G. A., "Structural Analysis of Ladder Frames under Torsion", Institution of Mechanical Engineers, Vol. 190, 1976.

5. Megson, T. H. G., Ergatoudis, J. and Nuttall, J., "Partially Restrained Warping of Open and Closed Section Thin-Walled Beams", Proc. of the International Conference on Thin-Walled Structures, University of Strathclyde, April 1979.

6. Oden, J. T., "Mechanics of Elastic Structures", McGraw-Hill Book Co., New York, 1967.

7. PAFEC 75, Manual for the Program for Automatic Finite Element Calculations, PAFEC Ltd., Nottingham 1976.

APPENDIX 2: Notation

A_R - area swept out by a generator, rotating about the centre of twist, from the point of zero warping to any point in cross-section
b - secondary beam flange width
d - secondary beam web depth
E - Young's modulus
G - shear modulus
J - torsion constant ($= \Sigma st^3/3$)
k - warping restraint factor
L - secondary beam length
n - perpendicular distance to any point in section wall from mid-line
R_d - secondary beam web depth/ main beam web depth
s - distance along mid-plane of a section
SCF - stress concentration factor
s_s - distance along section profile from centre of twist
T - applied torque
t - wall thickness
t_f - secondary beam flange thickness
t_s - main beam web thickness
t_w - secondary beam web thickness
t_x - secondary beam thickness (uniform)

w - warping displacement
z - longitudinal axis of beam
Γ - torsion bending constant ($= \int_{\text{section}} 4A_R^2 \, t \, ds$)
θ - angle of twist
μ - $\sqrt{(GJ/E\Gamma)}$
σ - partially restrained warping direct stress
σ_Γ^p - completely restrained warping direct stress
τ - shear stress
τ_Γ - partially restrained warping shear stress
$\tau^p_{St.V}$ - St. Venant shear stress
τ_Γ - completely restrained warping shear stress

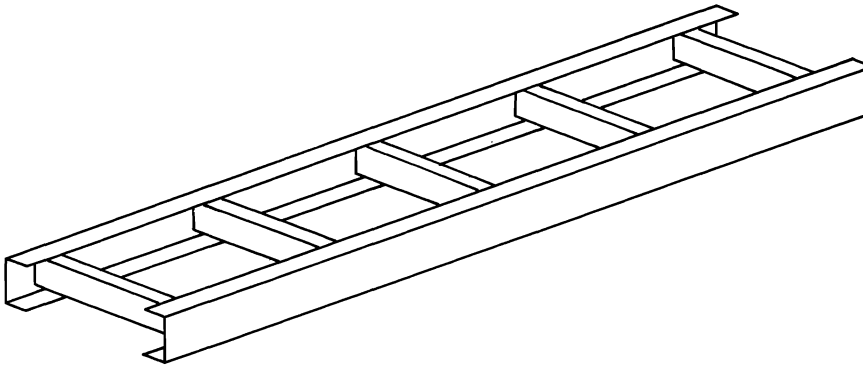

Fig.1 Typical ladder frame layout

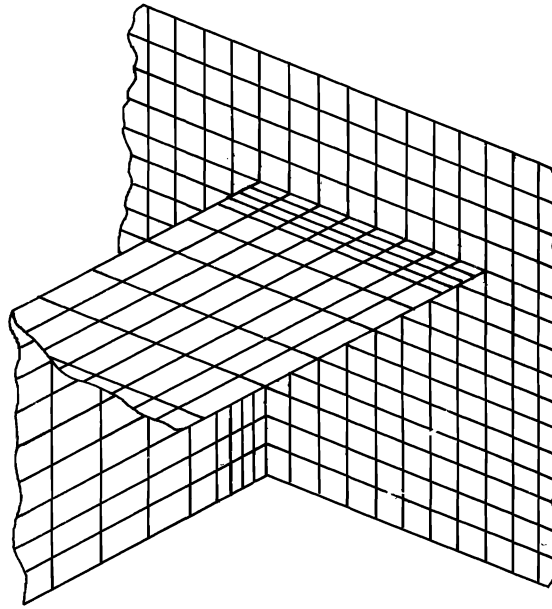

Fig.2 Finite element idealisation of a ladder frame joint

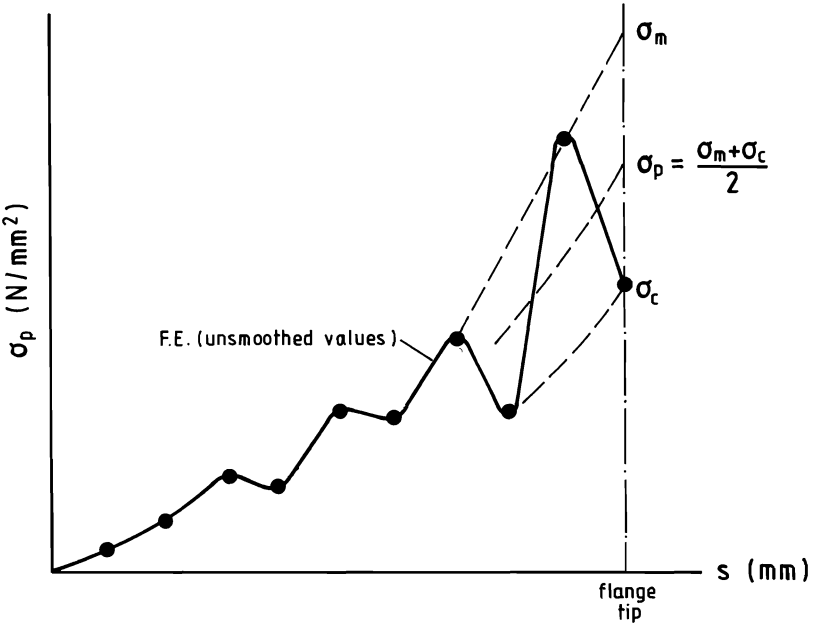

Fig. 3 Determination of flange tip surface stress

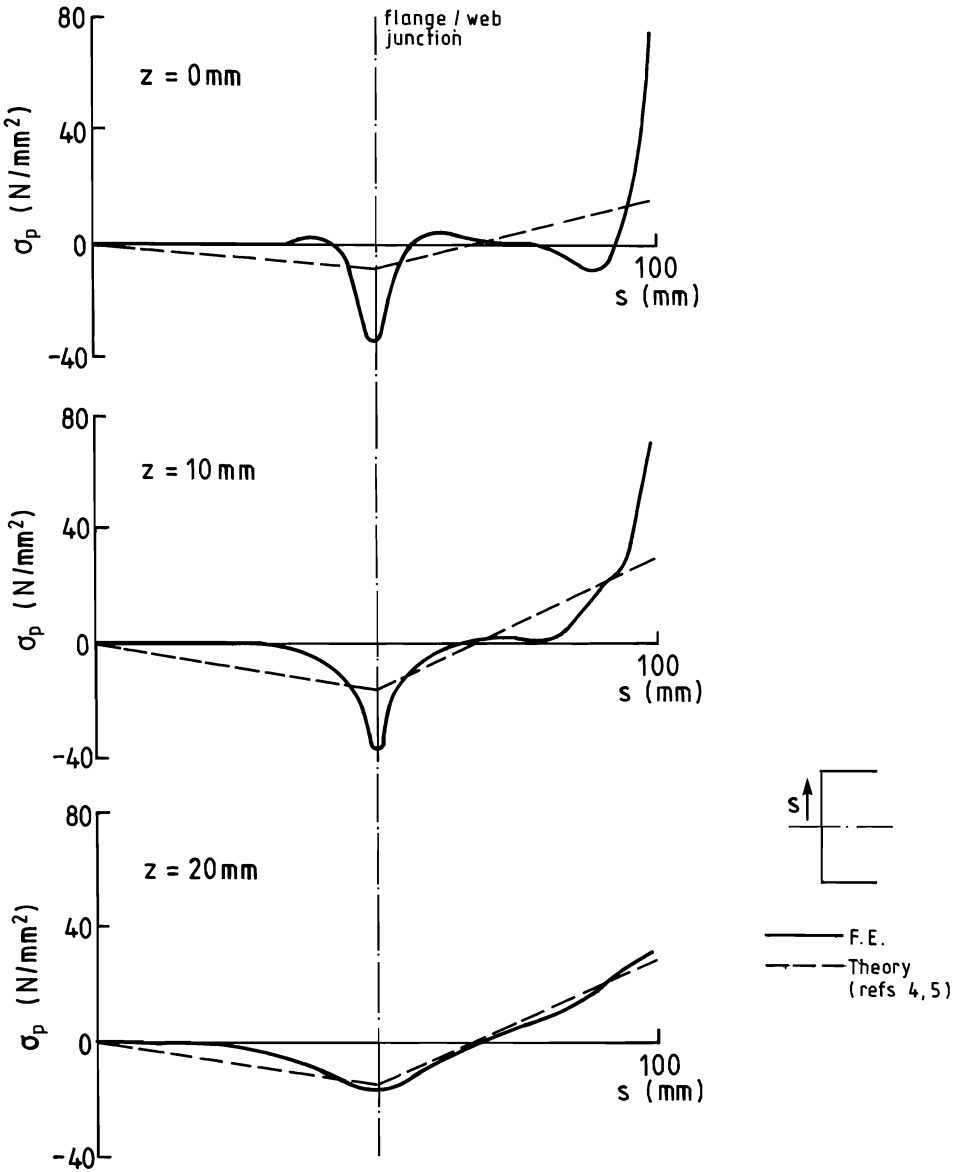

Fig. 4 Mid-plane axial constraint direct stress distribution round a channel section secondary beam (L = 300 mm, z is measured from the partially built-in end)

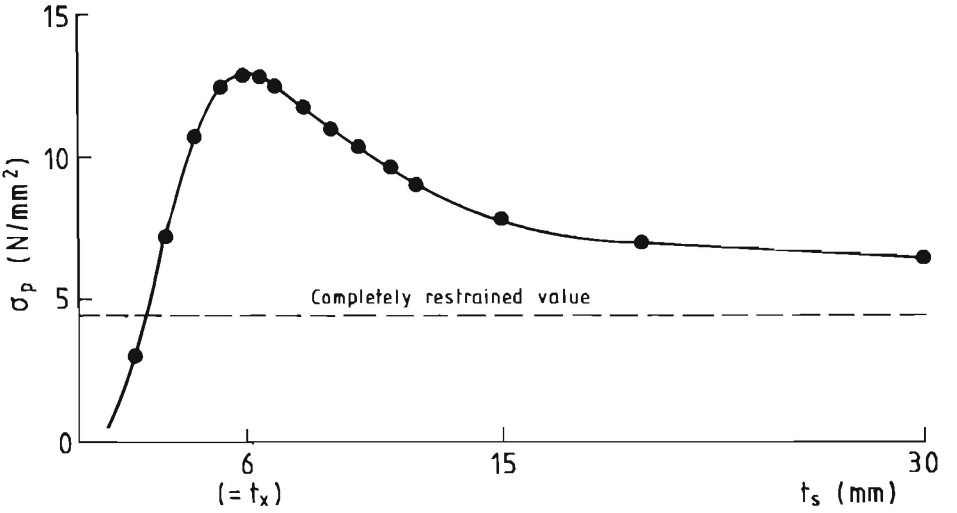

Fig. 5 Variation of mid-plane σ_p at flange tip (I-section secondary beam) at z = 0mm with main beam web thickness.

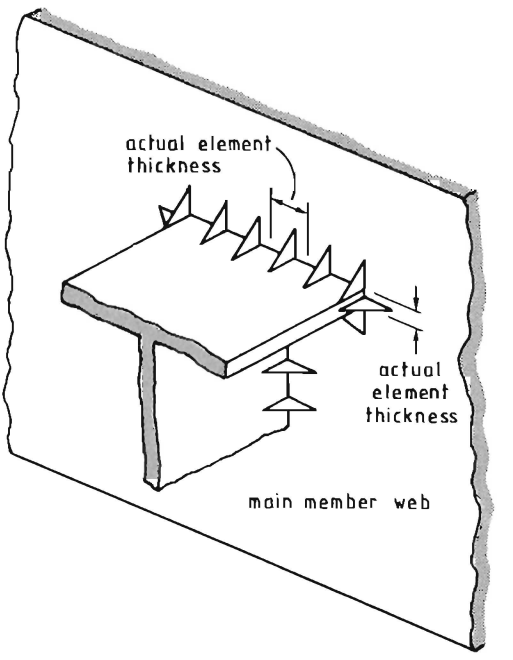

Fig. 6 Representation of fillet welds using finite elements

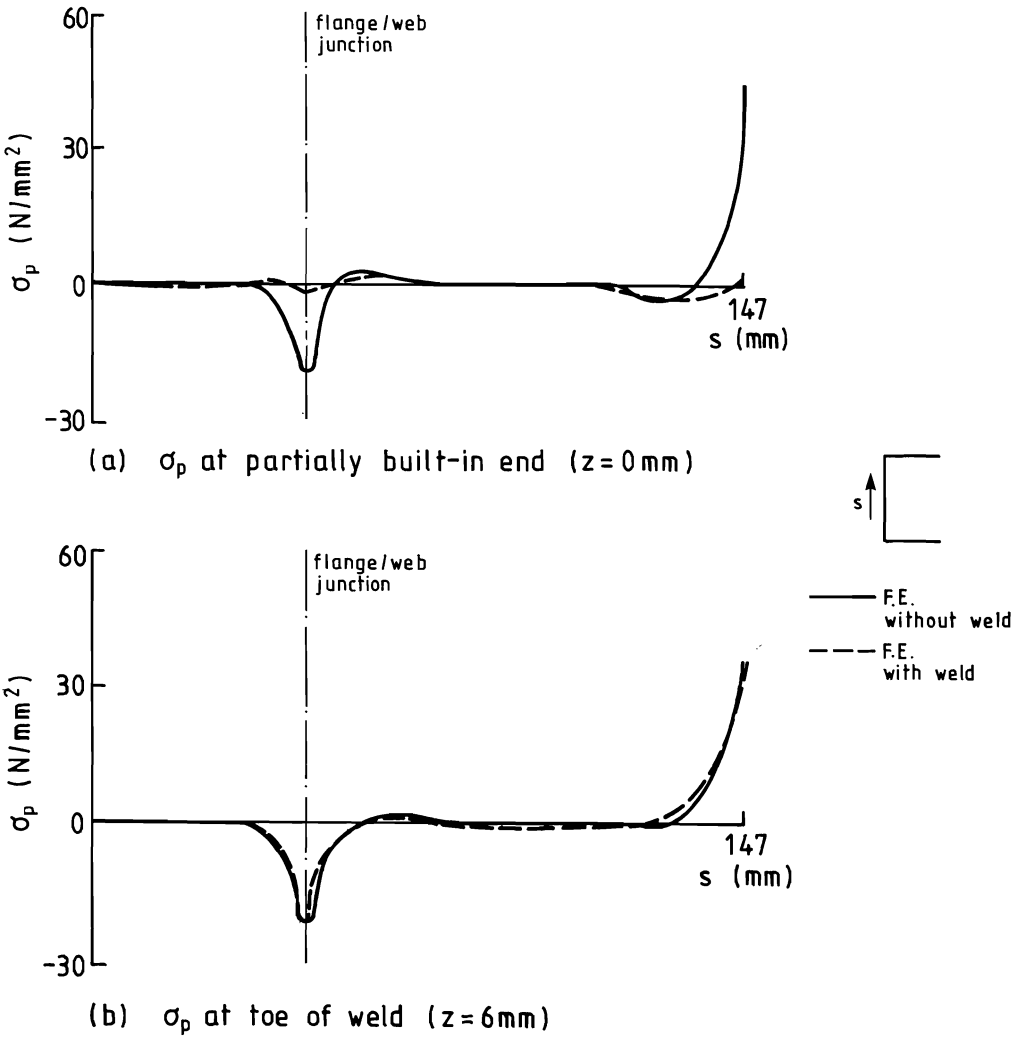

Fig. 7 Mid-plane axial constraint direct stress in a steel joint with and without fillet weld

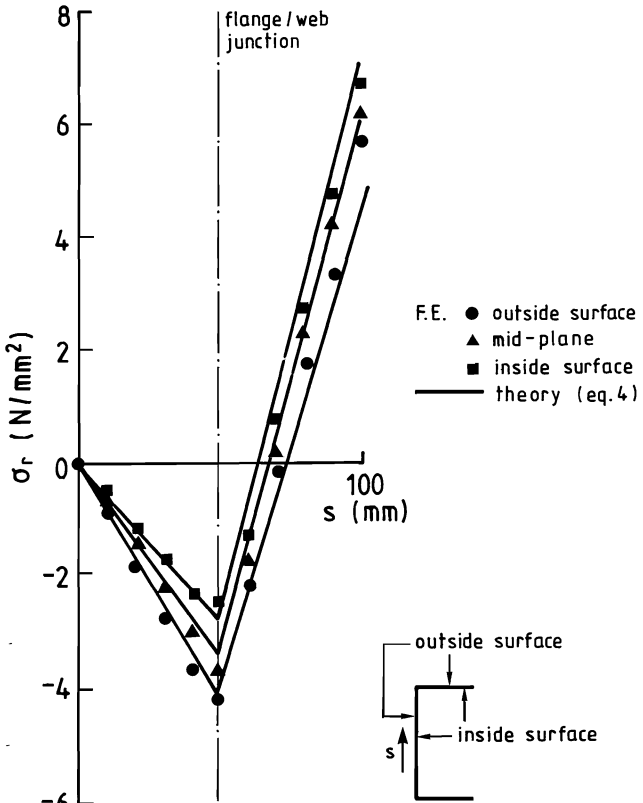

Fig. 8 σ_r across wall thickness at z = 150 mm. Completely restrained warping (channel section)

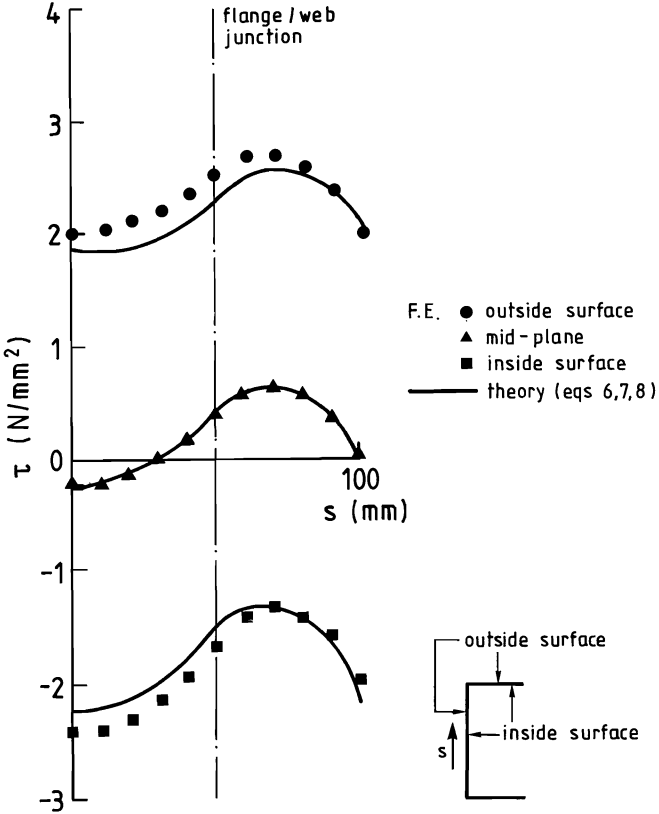

Fig. 9 τ across wall thickness at z = 150 mm. Completely restrained warping (channel section)

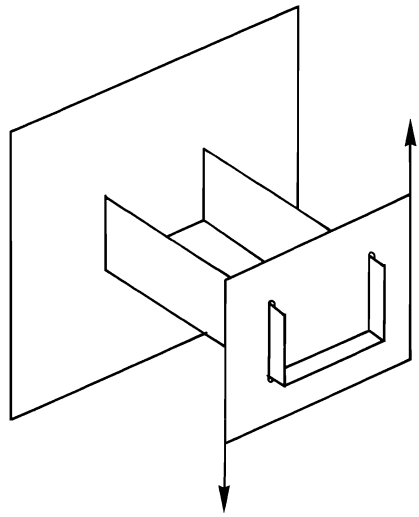

Fig. 10 Testing of glued perspex joints

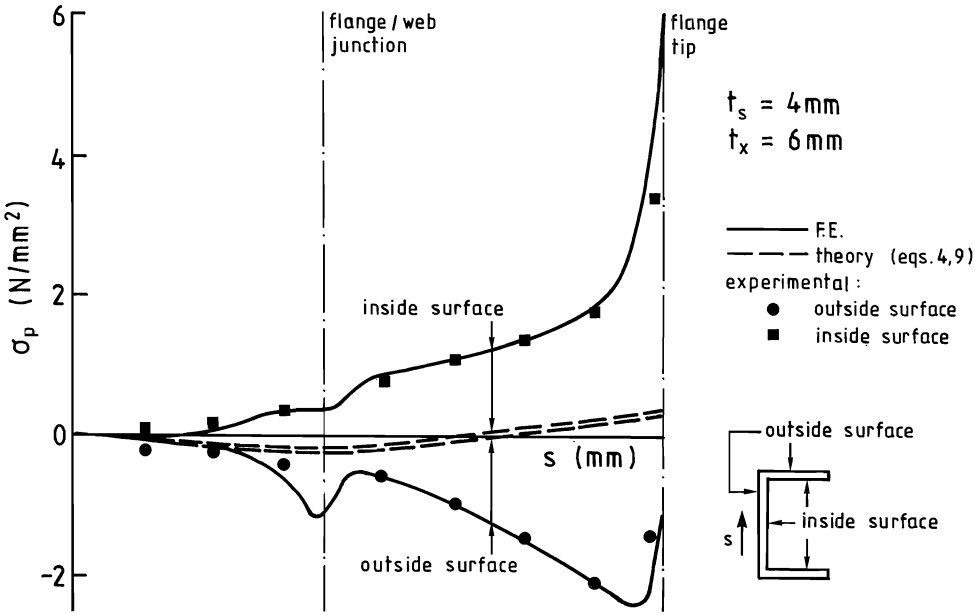

Fig. 11 Surface axial constraint direct stress distribution round secondary beam section (glued perspex joint)

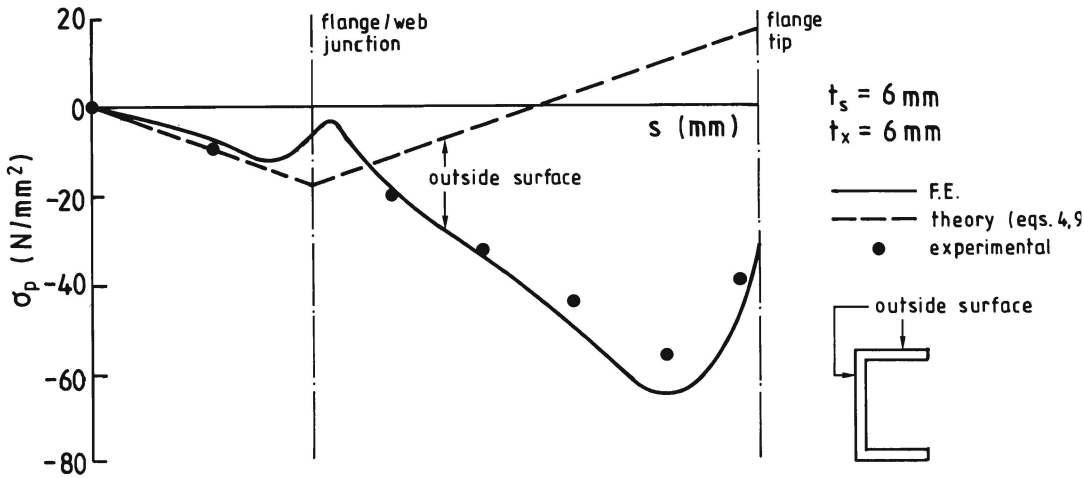

Fig. 12 Axial constraint direct stress at toe of weld in welded steel joint

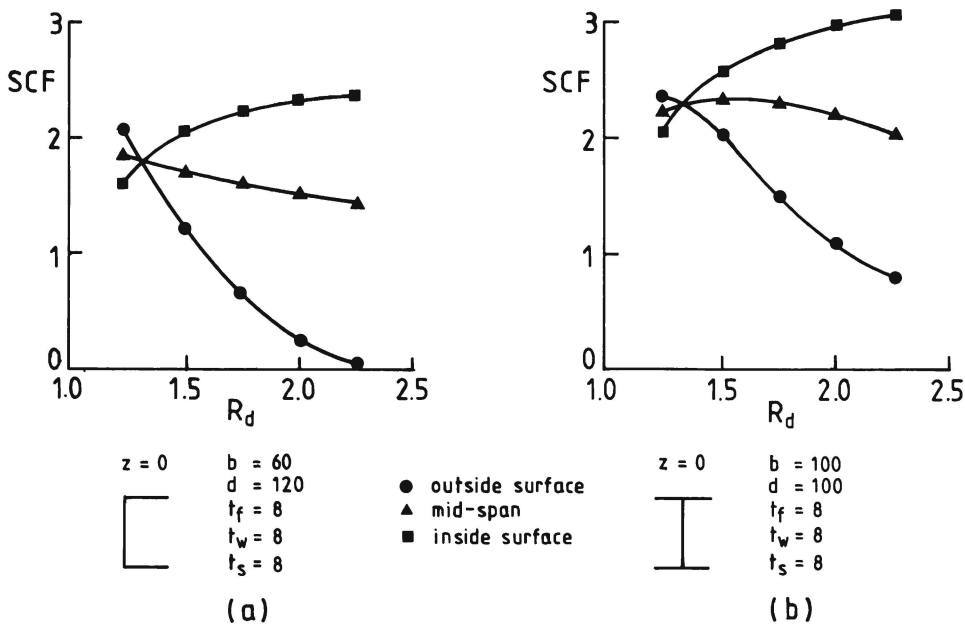

Fig. 13 Variation of SCF with R_d